Exp Astron (2015) 40:253–279
DOI 10.1007/s10686-014-9375-4

ORIGINAL ARTICLE

# JEM-EUSO: Meteor and nuclearite observations

**M. Bertaina · A. Cellino · F. Ronga · The JEM-EUSO Collaboration**

Received: 22 August 2013 / Accepted: 24 February 2014 / Published online: 3 April 2014
© Springer Science+Business Media Dordrecht 2014

**Abstract** Meteor and fireball observations are key to the derivation of both the inventory and physical characterization of small solar system bodies orbiting in the vicinity of the Earth. For several decades, observation of these phenomena has only been possible via ground-based instruments. The proposed JEM-EUSO mission has the potential to become the first operational space-based platform to share this capability. In comparison to the observation of extremely energetic cosmic ray events, which is the primary objective of JEM-EUSO, meteor phenomena are very slow, since their typical speeds are of the order of a few tens of km/sec (whereas cosmic rays travel at light speed). The observing strategy developed to detect meteors may also be applied to the detection of nuclearites, which have higher velocities, a wider range of possible trajectories, but move well below the speed of light and can therefore be considered as slow events for JEM-EUSO. The possible detection of nuclearites greatly enhances the scientific rationale behind the JEM-EUSO mission.

**Keywords** Meteors · Nuclearites · JEM-EUSO · Space detectors

M. Bertaina (✉)
Dipartimento di Fisica, Università di Torino, INFN Torino, via P. Giuria 1, 10125 Torino, Italy
e-mail: bertaina@to.infn.it

A. Cellino (✉)
INAF-Osservatorio Astrofisico di Torino, Strada Osservatorio 20, 10025 Pino Torinese (TO), Italy
e-mail: cellino@oato.inaf.it

F. Ronga (✉)
Istituto Nazionale di Fisica Nucleare - Laboratori Nazionali di Frascati, Via E. Fermi 40, 00044 Frascati, Italy
e-mail: francesco.ronga@lnf.infn.it

## 1 Introduction

JEM-EUSO, namely the proposed Extreme Universe Space Observatory on board the Japanese Experiment Module of the International Space Station (ISS) [1, 18, 36], is currently under study and is designed to be a great example of a multi-disciplinary mission. It will able to produce results of utmost importance for a wide and heterogeneous scientific community which includes theoretical and experimental physicists, high-energy astrophysicists, solar system specialists and experts of atmospheric phenomena. This unusually wide range of disciplines is certainly one of the major strengths of the mission.

Large networks of ground-based observing stations for the detection of meteor phenomena have been established in many countries all around the world over the years. Networks are currently active in middle-Europe (European Fireball Network [30]), Spain [37, 39], Australia [10], and Canada [40]. The networks include both amateur and professional observers, using a variety of detectors, ranging from old-fashioned photographic cameras to state-of-the-art electronic detectors (CCD and digital video recorders). In addition, meteors are also detected at radio wavelengths [42, 43].

Although all the aforementioned ground-based facilities have many merits and have been successfully operational for many years, this does not mean that they are without limitation. First, the volume of sky observable by any one observatory is forcedly limited. Even in the best cases, existing ground-based networks for meteor observations, like the European Fireball Network, cover less than 1 % of the Earth's surface [30]. Second, the efficiency of optical meteor observations from the ground is seriously affected by adverse weather conditions – primarily the presence of clouds. The ideal goal of ground-based networks is the simultaneous detection of meteors and fireballs [1] from different stations. The goal is to be able to obtain a trigonometric reconstruction of the observed paths of meteoroids moving across the atmosphere, and to obtain deceleration profiles. Whenever the astrometric accuracy can be good enough, the actual path of possible surviving fragments may in principle be computed in such a way as to make it possible the recovery of meteorites on the ground. Due to the above-mentioned problems of limited sky coverage and bad weather, however, this ideal goal of ground-based networks has been rarely achieved for many years [30].

In principle, meteor events are best detected from space-based facilities [15]. This includes both the light emitted at visible wavelengths, and the thermal infrared radiation produced by the heating of the meteoroid material as it moves through the atmosphere. Infrared observations are certainly possible from the ground, but space-based detectors work much more efficiently in the infrared. This is trivially true when sources are above the atmosphere, but it still holds also for phenomena occurring in the upper atmosphere. Space-based infrared detectors suffer far less atmospheric extinction compared to ground-based facilities.

[1] The term *fireball* usually indicates extremely bright meteors, as will be explained below.

Space-based sensors have a number of other obvious advantages. They can cover wider areas of sky and, being located above the atmosphere, are not limited by weather conditions. In spite of these advantages, meteor and fireball detections from space have not been routinely reported in the past for a long time. Only recently the situation has started to improve noticeably, as shown by a couple of recent fireball events producing meteorites, namely Almahata Sitta [24] and Chelyabinsk [35]. The reason of a general lack of detection reports in past years was mainly due to the fact that many satellites are equipped to monitor phenomena occurring over much longer time scales than the few seconds which generally characterize meteor phenomena. Consequently, in many cases meteor events were not detected or recorded. On the other hand, satellites equipped with sensors suited for fireball detection have been operative since a long time, but they have generally (though not exclusively) had military purposes which do not include the scientific study of meteor events. The data produced by these detectors are usually classified and not made public.

After decades of ground-based activities, the time has come to plan the development of a new generation of dedicated, space-based facilities for the detection of meteors. JEM-EUSO is a prime candidate to become the first example of a space mission to produce important data for meteor studies, including primarily the determination of the meteor flux in a wide range of magnitudes and the measurement of meteor light curves, as well as, possibly and in some cases at least, a computation of the original heliocentric orbits of the meteoroids, as will be noted in following section. All the above properties are important to improve our knowledge of the inventory of meteoroids on orbits which can cross the Earth's orbit, the main physical properties of these bodies (including their size distribution and likely compositions), their origin and likely dynamical evolution.

It should also be noted that a very interesting by-product of the observations of meteor-like objects is the possibility of detecting super-heavy exotic particles that may be important components of the so-called dark matter in our Universe. In particular, some neutral strange-quark material particles, called nuclearites. These can produce UV emissions which could be comparable to meteor signals. We estimate that the large aperture of the JEM-EUSO telescope will provide an improvement of approximately one order of magnitude over the existing limits for the detection of high-mass nuclearites in just 24 hours of operation.

This paper is organized as follows: in Section 2 we summarize some relevant notion concerning meteors. In Section 3 we do the same for nuclearites. In Section 4 we describe in general terms the focal plane assembly of JEM-EUSO, in order to explain the general principles of data acquisition. In Section 5 we describe the body of simulations which have been carried out so far in order to develop a reliable strategy for the observations of slow events, primarily meteors. A summary of our results is given in Section 6, in which we focus also on nuclearites. We also explain why we believe that the general observing strategy developed for the observation of meteors is, in principle, suitable for the detection of nuclearites, too. The general conclusions of our current work and the perspectives for future refinements are discussed in Section 7.

## 2 Brief outline of meteor phenomena

The presence of a large population of micro-meteoroids in space is indicated by the existence of zodiacal light, consisting of sunlight reflected by small dust particles orbiting the Sun near the ecliptic plane.

The vast majority of the extraterrestrial bodies hitting the Earth are in fact sub-mm dust particles, which can become visible as meteors in the night sky.

The initial and final heights of the phenomena of meteor ablation (corresponding to the part of the trajectory in the atmosphere where the object becomes luminous) are very variable (interested readers are addressed, for instance, to Fig. 6 in [29]). As a first approximation, we can state that typical initial heights at which meteors become visible are between 75 and 120 km, while the end points are generally at heights between 30 and 100 km. The duration of the events range typically between 0.5 and a few seconds. These are therefore slow events for JEM-EUSO, as we will see below. The brightness varies over a huge interval, including events which are not visible to the human eye, up to extremely bright (and much more unusual) events, which may well be visible even during day time.

Approximately 75 % of meteor events are sporadic, whereas one fourth of the events are genetically associated in a number of meteoroid streams which produce meteor showers in well defined epochs of the year. This is due to the fact that each meteoroid stream is formed by bodies with very similar orbits, likely produced by low velocity ejection from a common parent body, typically a comet. Many known meteor showers (the Lyrids and Perseids, for example) are known to be associated with a parent comet. In the case of the Geminids, the parent body is an object previously classified as an asteroid, (3200) Phaeton. In recent years there has been increasing evidence that, at least in a few cases, the progenitor of some meteor stream can be some near-Earth asteroid (see below), rather than a comet [23, 38]. However, it is also believed that at least in some cases the supposed parent asteroids are most likely extinct comets [5, 6].

The population of small solar system bodies with orbits sweeping the region of the inner planets does not include only micro-meteoroids. Much larger bodies, though less abundant, do exist. It is known that, apart from comets, a population of so-called near-Earth asteroids (NEA) have orbits partly or totally interior to the orbit of Mars. The size distribution of the NEAs is described by a power-law (smaller objects being increasingly more abundant). It is currently estimated that about 1000 NEAs with sizes of the order of 1 km or larger exist. The number of bodies with sizes of some tens of meters should be of the order of 1 million. Figure 1 shows the estimated NEA size distribution as it was presented a few years ago in the NASA Report to the US Congress, *Near-Earth Object Survey and Deflection Analysis of Alternatives*. Note that the figure shows, in addition to the size and expected number of objects (both in log scale), estimates of the absolute magnitudes and impact frequencies of objects of different sizes, as well as an estimate of the delivered impact energies in the event of collision with our planet.

It is important to underline here that Ortiz et al. [31] have studied sporadic impact flashes on the Moon and estimated the impact rate of large meteoroids (0.1-10 $m$ in size) on the Moon and the Earth to be at least one order of magnitude higher

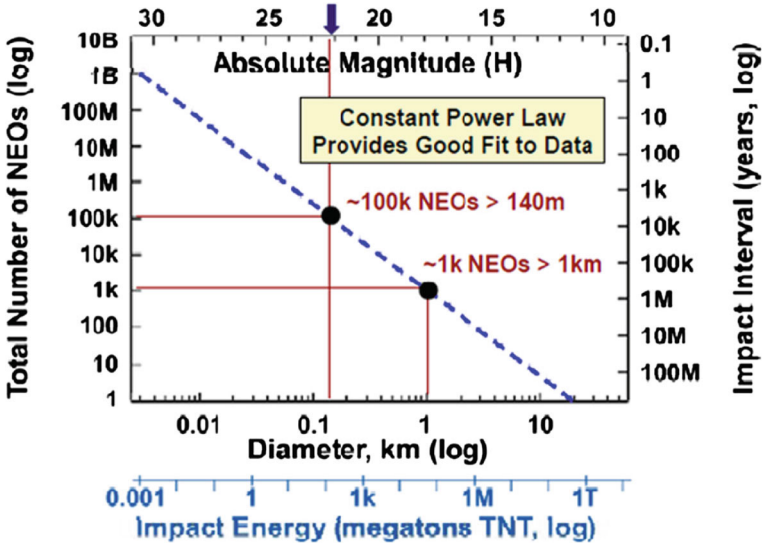


**Fig. 1** The size and absolute magnitude distributions of near-Earth objects according to the 2007 NASA Report to the US Congress (for a definition of the absolute magnitude of asteroids, see the text)

than the frequencies presented in the NASA report. Lunar-monitoring results are also consistent with a possibly enhanced frequency of terrestrial airbursts produced by impactors tens of meters in size like the recent Chelyabinsk event [11] and other events recently detected in remote locations by the infrasound network. Most such outbursts were unnoticed in the past. This is also another good reason to promote a global monitoring of superbolides from space in order to improve available statistics and better assess the impact hazard due to small asteroids.

Note also that the absolute magnitude of an asteroid is defined as the visual (that is, measured in the standard $V$ filter) magnitude that would be measured if the object was seen at unit distance from both the Sun and the observer, under conditions of ideal solar opposition. This definition takes into account that the apparent brightness of these objects varies (trivially) as a function of distance, and (less trivially) as a function of illumination conditions. It is also noteworthy that in the case of meteors, another definition of absolute magnitude holds: in particular, the absolute magnitude of a meteor is the apparent magnitude which would be measured by a ground-based observer if the meteor was seen at the zenith and at a distance of 100 km above the observer. It is clear that the apparent brightness of a meteor depends on the distance, and also greatly upon the atmospheric absorption, which changes at different angles from the zenith and under varying atmospheric conditions.

Objects with sizes of the order of some tens of meters or larger are called asteroids, while the term meteoroid applies to smaller sizes. These are very faint objects, that are barely detectable by means of telescopes, so they reveal their existence mostly when they enter the Earth's atmosphere and become bright. In fact, whenever the

impacting body's size is larger than some limit depending on the entry velocity vector (about 20 cm for a velocity entry of 15 km/sec from the zenith direction), the resulting meteor can be extremely bright. When the apparent brightness of a meteor reaches a magnitude around $-4$ or brighter at visible wavelengths, it is called a *fireball*, or *bolide*, corresponding to impactor masses which may vary from approximately 0.1 up to 1000 kilograms. When the magnitude reaches or exceeds $-17$, corresponding to impacting bodies of mass greater than 1, 000 kg, the term *superbolide* is also used [15].

Meteoroids hit the Earth's atmosphere at hypersonic velocities ranging from about 12 to 72 km/sec. Depending on the entry velocity and the mass of the meteoroid, or micro-meteoroid, different phenomena are then produced. All of them, are a consequence of the conversion of the kinetic energy of the impacting body into other forms of energy. As a general rule, a release of ions and free electrons occurs along the meteoroid path through the atmosphere. This is due to collisions between the atoms and molecules in the atmosphere and the surface of the meteoroid. Visible light is then produced by de-excitation of these ions. In less frequent cases, corresponding to the most energetic events, additional detection of acoustic and infrasonic blast wave effects is also possible.

The most common outcome of the entry of a meteoroid into the Earth's atmosphere is the meteor phenomenon, which is produced by tiny bodies of sizes which, depending on the entry velocity, are typically above a fraction of a *mm* [14]. After a preliminary heating at heights between 300 and 100 km (preheating phase), a phase called *ablation* follows, in which the surface material begins to sublimate and a layer of hot vapor is produced around the body. This is heated up to temperatures well in excess of 4000 K. Excited states are produced in the constituent ions of this surrounding layer, causing the emission of light at characteristic wavelengths as they lose energy during de-excitation. This phenomenon occurs in the range 75 to 120 km. The process continues until the body is completely disintegrated, generally at heights between 30 and 100 km, after traveling a distance which may range from several kilometers up to few tens of kilometers. A typical meteor ends up losing all of its mass, though not radically changing its velocity. The latter generally decreases by an amount between several percent up to a few tens of percent, depending on the range of heights covered by its path through the atmosphere (the attrition becoming larger at lower heights), and depending also in a more complicated way on the shape (cross section) of the body itself. The duration of the phenomenon is generally between 0.5 and 3 seconds. Because ions and free electrons are produced in an ionized column along the path of the body in the atmosphere, it is also possible to detect these events by means of radar techniques.

In particular conditions, when the impactor is sufficiently large and resistant, the meteoroid can survive the phase of ablation, and is slowed down until it reaches a state of free fall. A phase of so-called dark flight can be reached, and what remains of the meteoroid eventually reaches the ground as a *meteorite*. In extreme cases the meteoroid can be so large that its velocity is only weakly reduced by interaction with the atmosphere. No dark-flight free fall phase occurs and the body hits the ground violently at hypersonic speed producing an impact crater, or possibly a tsunami in the case of ocean impact. These extremely rare events, which have been responsible for

episodes of mass extinction of the Earth's biosphere in the past, are clearly beyond the scope of this article.

According to [15], over average timescales of the order of 100 years, most of the mass delivered to the Earth by colliding interplanetary bodies comes from superbolides with individual masses between $10^3$ and $10^7$ kg, and typical sizes of the order of 10 meters. Bodies in this size range are the least known population of minor bodies in our Solar system [14]. The number of events involving bodies in this size range is thought to be larger than 50 events per year, justifying a systematic observational effort.

Apart from the very rare and hugely destructive impacts producing craters on the Earth's surface and regional or global devastation, bolides and superbolides represent the most spectacular events of collision with extraterrestrial material.

For several decades a significant effort has been made in order to detect and record the maximum possible number of these events. The general purposes are the determination of the three-dimensional entry velocity vector of the bodies, in order to derive their pristine heliocentric orbits; the determination of their composition, derivable from spectra; the study of ablation mechanisms based on the observed meteor lightcurve.[2] Another major goal is to record the path in the atmosphere in order to compute the likely regions where meteorites might be found. The derivation of the inventory and size distribution of the bodies which can intersect the orbit of the Earth with a non-zero probability of collision with our planet, has been a high priority task of modern Planetary Science for a long time. Apart from obvious considerations of mitigating the impact hazard for the terrestrial biosphere, this is also a challenging theoretical problem, with important implications for our understanding of the orbital and physical evolution of the minor bodies of our Solar System.

At much smaller scales, typical of micro-meteoroids, the inventory of the population and the typical flux of Earth impactors is even more difficult to determine. Some estimates have been made based either on the observed numbers of micro-craters on the surface of the Moon, or on spacecraft-based measurements [20]. Figure 2, adapted from a figure in [20], shows a plot of the expected number of micro-meteoroid impacts per second occurring in the JEM-EUSO FoV as a function of micro-meteoroid mass. At very small masses some discrepancies exist between existing models, but it is clear that the number of events is, in any case, expected to be very high. According to Fig. 2, the number of expected events by micro-meteoroids with masses of 0.001 g in the JEM-EUSO FoV is of the order of 1 per second. The apparent brightness of these events is faint, however. To detect them it will be necessary to exploit the limited intervals of time when JEM-EUSO surveys very dark regions.

We also want to note that, apart from purely scientific issues, a space-based system for fireball surveillance might also have more immediate practical purposes. For instance, it is conceivable that the cloud of dust or smoke trail released by an energetic fireball could potentially be a hazard for aircraft for some time after the

[2]The meteor lightcurve is the recorded variation of the meteor brightness as a function of time

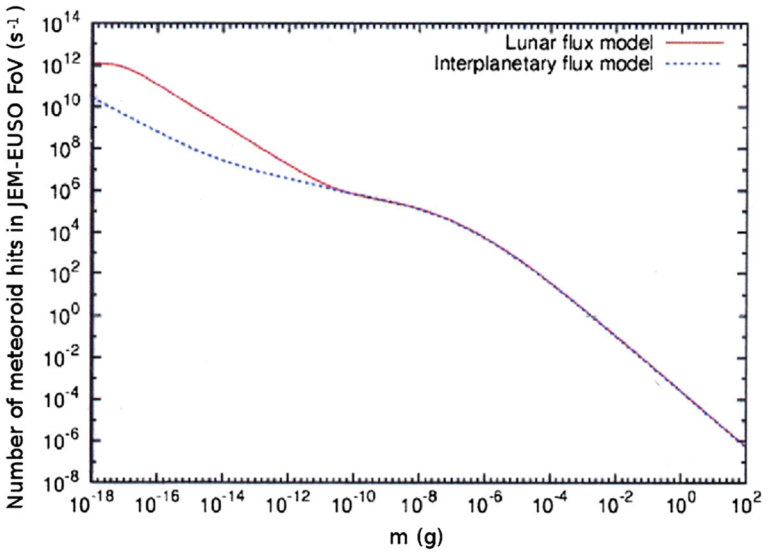


**Fig. 2** Number of micro-meteoroid impacts expected per sec in the JEM-EUSO FoV as a function of impactor mass in grams. Figure adapted from [20]

event. For these and other reasons, a prompt detection of these events could be of the highest importance for mitigation of potential dangers for human beings in such circumstances.

## 3 Brief outline of nuclearites and other super-heavy particles

During the last decade significant experimental and theoretical effort has been devoted to the problem of dark matter (DM). There is compelling evidence of the existence of DM at all astrophysical length scales. Astrophysics and "standard cosmology" require 84 % of matter to exist in the form of DM. The local DM density in our galactic halo should be of the order of $0.3\,\mathrm{GeV/cm^3}$, and the DM speed should have values typical of galactic halos, around 270 km/sec. Many DM candidates have been proposed in the literature [8]. Studies of the formation of structures in the Universe, and the standard cosmology models indicate that most DM should be cold, *i.e.*, it should not be relativistic at the onset of galaxy formations. This excludes light particles as neutrinos as possible candidates to contribute in a significant way to the DM.

Supersymmetry predicts many new supersymmetric particles, among which neutralinos are the lightest super-particles predicted by the theory. The neutralino is an example of a "weakly interacting massive particle" (WIMP). Such particles have been the most promising DM candidates for a long time, and have been the targets of most experiments designed to carry out a direct search for DM. The current cross section sensitivity in DM experiments is as small as $10^{-8}$ pbarn in a mass range from a few GeV to a few TeV [7]. This sensitivity is already sufficient to exclude a fraction

of the regions predicted by supersymmetric models. LHC experiments could directly detect DM particles produced in $p$-$p$ collisions. So far, however, there is no evidence of supersymmetric nor generic new particles in LHC data in the TeV range up to $\sqrt{s} = 8\,\text{TeV}$.

From a pessimistic standpoint, those negative results could suggest that DM particles have only gravitational interactions. In this case, due to their very small cross section, a detection with particle detectors would be impossible. Another possibility is that DM particles could be much heavier than the few TeV mass reached by current experiments. The possible existence of super-heavy dark matter particles, sometimes called Wimpzillas, would have interesting phenomenological consequences, including a possible solution of the problem of cosmic rays observed above the GZK cutoff. The literature is full of exotic names for such particles: CUDOs [25], Q-balls, mirror particles, CHArged Massive Particles, (CHAMPs), self interacting dark matter, cryptons, super-weakly interacting dark matter, brane world dark matter, heavy fourth generation neutrinos, *etc.* (see the references listed in [8]). Even if strongly interacting, these objects could remain 'dark' due to their large mass-to-surface area ratio and correspondingly low number density required to explain the observed DM mass density.

More recently, composite objects consisting of light quarks in a color superconducting phase have been suggested. In addition, super-heavy DM anti-quark nuggets could exist and could perhaps solve the matter-antimatter asymmetry [19]; the detection of such anti-quark nuggets by cosmic ray experiments is discussed in [26]. The energy loss predicted for super-heavy DM particles varies in different models, but it is likely that such particles could be confused with meteors, since their expected velocity, 270 km/sec, is higher than high-end tail of the meteor velocity distribution, but not dramatically.

Here, we will focus our attention only on one possible kind of very massive particle called the "nuclearite". It consists of neutral matter including a strange quark among its constituents. We make this choice because nuclearites are an example of particles already searched for by other experiments, and for which we could compute the performance of JEM-EUSO as a possible detector.

Nuggets of Strange Quark Matter (SQM), composed of approximately the same numbers of up, down and strange quarks could be the true ground state of quantum chromodynamics [2, 41]. SQM nuggets could be stable for all baryon numbers in the range between ordinary heavy nuclei and neutron stars. They may have been produced in the early Universe. As the strange quark is massive compared to almost massless up and down quarks, surface tensions lead to the suppression of a few s quarks. Thus, SQM should have a relatively small positive electric charge compared to that of heavy nuclei [17]. Macroscopic quark nuggets, neutralized by captured electrons, are called nuclearites. In the case of small baryon numbers ($A \leq 10^6$), assumed to be quasi totally ionized, they will be called strangelets. Upper limits for the concentrations in lunar soil samples of strangelets in a range of possible values of mass and nuclear charge have been obtained by [21]. There have been also several concerns about the SQM hypothesis; one was raised in 1999, when heavy-ion collisions between gold nuclei were produced at the Brookhaven National Laboratory (USA) and again before the LHC was run with heavy ions: negative strangelets would

attract positive nuclei and could ingest them sequentially, resulting in the consumption of the entire planet. Fortunately, however, there are theoretical considerations suggesting that negative strangelets are unlikely to exist [9, 16].

According to [17] nuclearites are considered to be large strange quark nuggets, with overall neutrality ensured by an electron cloud which surrounds the nuclearite core, forming a sort of atom. Nuclearites with galactic velocities are protected by their surrounding electrons against direct interactions with the atoms they might hit.

As a consequence, the principal energy-loss mechanism for a nuclearite passing through matter is atomic collision. For a massive nuclearite the energy-loss rate is:

$$\frac{\mathrm{d}E}{\mathrm{d}x} = -A\rho v^2 \tag{1}$$

where $\rho$ is the density of the traversed medium, $v$ the nuclearite velocity and $A$ is its effective cross-sectional area. The effective area can be obtained by the nuclearite density $\rho_N$. For a small nuclearite of mass less than 1.5 ng, the cross-sectional area $A$ is controlled by its electronic atmosphere which is never smaller than $10^{-8}$ cm:

$$A = \begin{cases} \pi \cdot 10^{-16}\,\mathrm{cm}^2 & \text{for } m < 1.5\,\mathrm{ng} \\ \pi\left(\dfrac{3m}{4\pi\rho_N}\right)^{2/3} & \text{for } m > 1.5\,\mathrm{ng} \end{cases} \tag{2}$$

where $\rho_N = 3.6 \cdot 10^{14}\,\mathrm{g/cm}^3$ is the nuclearite density and $m$ its mass.

According to 1, nuclearites having galactic velocity and mass exceeding $10^{-14}$ g penetrate the atmosphere, while those heavier than 0.1 g pass freely through an Earth diameter. Equation 1 has been used by [17] to compute the amount of visible light emitted in the atmosphere, assuming that the light is emitted as black-body radiation from an expanding cylindrical thermal shock wave and to compute therefore the apparent magnitude as defined for meteors.

The efficiency of the light emission due to the black body radiation is inversely proportional to the medium density: this cancels the density dependence of the energy-loss and therefore in most of the nuclearite path in the atmosphere the light emission is constant with height. According to [17] the upper limit to the altitude ($h_{max}$) at which nuclearites effectively generate light is described by the following relation:

$$h_{max} = 2.7 \ln(m/1.2 \times 10^{-5}\ g)\ \ \mathrm{km} \tag{3}$$

and for altitudes less then $h_{max}$ the light emitted is constant. For the range of masses 0.1-100 g, $h_{max}$ is expected to be located between 24 km and 60 km.

It is clear that there are three important differences that can help to discriminate between nuclearites and meteors. The first is that the light emission of nuclearites is expected to be constant at $h \leq h_{max}$. The second is that a nuclearite of mass greater than 0.1 g can move upward and this is extremely unlikely for a meteor. The third is that the absolute value of the velocity is higher, with a maximum value of $\sim 570$ km/sec, while meteors are limited to $\sim 72$ km/sec.

Nuclearites and similar particles, for example neutral Q-balls [28], have been searched for using different approaches. The experiments can be characterized by the detection area ($S$) and by the minimum nuclearite mass that can be detected

($m_{th}$), usually computed for a speed of 270 km/sec. Many techniques, summarized in Table 1 have been used to detect nuclearites: acoustic emission due to the thermal shock in aluminum gravitational wave cylindrical detectors, damage in plastic materials like CR39, Makrofol or Lexan, light emission in oil or sea water, seismic waves induced by large nuclearites. Due to the uncertainties in the energy losses it is important to have different techniques to detect such exotic particles. Table 1 lists the different techniques and a representative experiment of each technique. It is not intended to be a comprehensive list of the experiments performed thus far in the search for nuclearites, but it is a reasonable summary of the state of the art in this field.

## 4 General description of JEM-EUSO payload and focal plane assembly

A general description of the JEM-EUSO telescope has already been given elsewhere in this volume. We recall here only the essential points related to the meteor and nuclearite discussion. The role of the JEM-EUSO telescope [27] is to act as an extremely-fast ($\sim \mu$s) and highly-pixelized ($\sim 3 \times 10^5$ pixels) digital camera with a large aperture (a diameter of about 2.5 m) and a wide field of view (FoV) of 60°. It operates in near-UV wavelengths ($290 - 430$ nm).

The optics focuses the incident UV photons onto the focal surface. The focal surface detector converts incident photons into electric pulses. The electronics counts the number of pulses in time intervals of 2.5 $\mu$s (Gate Time Unit - GTU) and records it. When a signal pattern is found, a trigger is issued. This starts a sequence which eventually transmits the signal data recorded within (and surrounding) a selected pixel region to the ground operation center.

The combination of 3 Fresnel lenses provides an angular resolution of 0.075°. This resolution corresponds to a linear size of approximately 550 m on the Earth's surface directly beneath the ISS located at an altitude above ground of about 400 km. The corresponding linear size at a height of 100 km above the ground, typical of meteor events, is about 400 m.

The Focal Surface (FS) of JEM-EUSO has a spherical shape approximately 2.3 m in diameter with about 2.5 m curvature radius, and is covered by $\sim 5,000$ multi-anode photomultiplier tubes (MAPMTs). The FS detector consists of Photo-Detector

**Table 1** Experimental techniques, locations, representative experiments, sensitive area and nuclearite mass thresholds computed for $v = 270$ km/sec

| Technique | Location | Experiment | $S$ (m$^2$) | $m_{th}$ (g) |
|---|---|---|---|---|
| Thermo-acoustic | sea level | [4] | $\sim 1$ | $10^{-13}$ |
| Damage | mountain 5230 m a.s.l. | [13] | 427 | $5 \cdot 10^{-14}$ |
| Light in oil | underground 3700 hg cm$^{-2}$ | [3] | $\sim$700 | $2 \cdot 10^{-10}$ |
| Light in water | underwater 2500 hg cm$^{-2}$ | [32] | $\sim 10^5$ | $2 \cdot 10^{-10}$ |
| Earth or Moon-quakes | Earth/Moon inner | [22] | $\sim 10^{11}$ | $\sim 10^4$ |

Modules (PDMs), each of which consists of 9 Elementary Cells (ECs). Each EC contains 4 units of MAPMT (Hamamatsu R11265-03-M64, 2 inches in size, with $8 \times 8$ pixels). A total of 137 PDMs are arranged on the FS. A Cockcroft-Walton-type high-voltage supply is used to reduce power consumption. It includes a circuit to protect the photomultipliers from sudden bursts of light, such as lightning or bright fireball phenomena.

The FS electronics system records the signals of UV photons generated by EECRs. A new type of front-end ASIC has been developed for this mission. It has both functions of single photon counting and charge integration in a chip with 64 channels. The FS electronics is configured in three levels corresponding to the hierarchy of the FS detector system: front-end electronics at EC level, PDM electronics common to 9 EC units, and FS electronics to control 137 units of PDM electronics. The anode signals from the MAPMT are digitized for each GTU and held in ring memory to wait for a trigger assertion. After the trigger, the data are sent to control boards. JEM-EUSO uses a hierarchical trigger method to reduce the data rate of $\sim 10\,\mathrm{GB/s}$ down to 297 kbps, required for transmission from the ISS to the ground operation center.

## 5 Simulations

### 5.1 Meteor simulations

A very simple model of meteor phenomena has been preliminarily developed in order to make it possible to carry out a campaign of numerical simulations aimed at analyzing the kind of signals which may be produced on the JEM-EUSO focal plane in a variety of possible observing scenarios.

One thing to bear in mind is that meteor phenomena are extremely variable in many important respects, including duration, brightness, brightness variation, speed and trajectory of the impacting body. Any model aimed at exploring the space of parameters, must therefore be quite flexible.

In a first preliminary version, the model assumes that a meteor phenomenon occurs at some instant, corresponding to a given initial height $h_{beg}$ (expressed in km) of the meteoroid. A cartesian reference system is defined, having its origin on the Earth's surface directly below the meteoroid at the instant $t = 0$. The $(x, y)$ plane of the coordinate system is parallel to the Earth's surface at the origin so that at $t = 0$, the meteoroid has the coordinates $(0, 0, h_{beg})$. For the sake of simplicity, it is assumed that JEM-EUSO has a constant height of 400 km. The direction of the $x$ axis is chosen to be coincident with the direction of the horizontal motion of JEM-EUSO, which is assumed to be linear and uniform. These assumptions are simplistic, but they are reasonable for describing events which have durations which do not exceed a few seconds. At $t = 0$, therefore, the coordinates of the JEM-EUSO focal plane are assumed to be $(x_0, y_0, 400)$. The initial $x_0$ and $y_0$ coordinates are chosen randomly or selected by the operator, but in any case a control is done in order to exclude the possibility that the simulated event could be outside the cone of observability of JEM-EUSO.

The model assumes an initial velocity vector for the meteoroid, and a given total duration for the event. Both the velocity and the duration can be chosen at random (within realistic ranges) or provided as inputs.

The variation of the brightness of the meteor as a function of time, or the meteor lightcurve, is also chosen randomly, or provided as an input. Since the shape of the lightcurve can be highly variable in the real world, the model adopts a very flexible approach, representing it with a polynomial of $9^{th}$ degree. In most practical applications performed so far, simulated lightcurves look reasonably realistic, taking into account the large intrinsic variability of the phenomenon, as shown, for instance, in the analysis by [33]. Moreover, since it is known that real meteors can exhibit one or more secondary bursts, the model includes the possibility to simulate one secondary burst, occurring at some instant before the end of the event, and having a morphology which is also represented by a degree 9 polynomial (again, fixed or randomly chosen).

Having selected the above parameters, the computations executed by the numerical simulator are trivial. At each time step, generally chosen to be equal to $10^{-3}$ sec, the position and brightness of the meteor are computed, and the fluxes reaching the JEM-EUSO focal plane, taking into account the varying distance from the detector, are then computed. The magnitudes are converted to photo-electrons per GTU. The varying position of the signal on the focal plane at different time steps is also computed. The same overall computation is also done for a hypothetical ground-based observer located at the origin of the coordinate system defined above.

In this way, a large variety of possible cases can be modeled. An example is given in Fig. 3. The results of such simulations can be used to develop an overall strategy of JEM-EUSO observation of slow events. In particular, we have so far preliminarily analyzed the possibility of deriving a correct identification of the events by adopting different triggering techniques, and considering meteor events with a variety of possible brightness, observed in different background conditions. It should be noted that the meteor simulator is also useful to simulate the signals produced on the focal plane by sources fixed on the ground, so mimicking what happens when urban

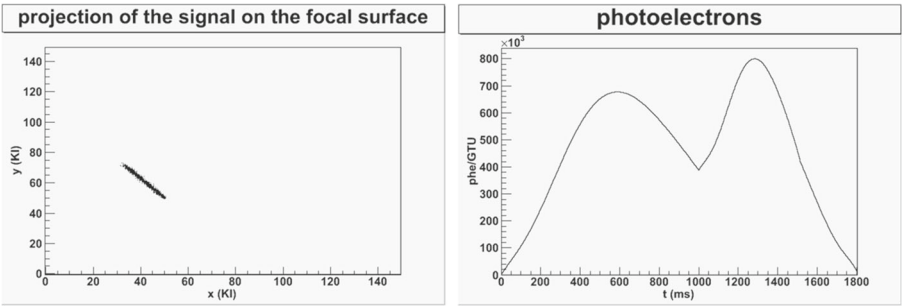


**Fig. 3** Example of meteor signal computations carried out using the simulation described in the text. The left panel shows the resulting path of the signal in the focal plane, while the right panel shows the simulated lightcurve, including a secondary burst occurring at $t \simeq 1000$ msec

agglomerations enter the field of view. Thanks to its flexibility, the meteor simulator allows also the generation of nuclearite tracks with their specific light profiles.

The simulation work carried out so far has still been fairly limited, but the results have been positive, and suggest that JEM-EUSO could detect meteors down to absolute visual magnitudes of the order of $5 - 6$, a limit which in absolute terms is not superior to the performance of the best ground-based facilities, but which becomes very interesting for meteor science by considering the large field of view and high duty cycle of the JEM-EUSO detector. Moreover, the detection of faint meteors, as interesting and useful as it may be, is probably not as important as a systematic and efficient detection of brighter events, including fireballs, which may be visible even in observing conditions far from optimal for cosmic rays detection. For bright events, the possibility of having also at disposal simultaneous detections from ground-based observing networks will be extremely useful. This would allow us to derive accurate $3D$ trajectories for these objects, from which the original meteoroid orbits, and possibly the coordinates of meteorite impact locations for objects sufficiently large and resistant to reach the ground, could be computed.

In its current version, the meteor simulator developed for JEM-EUSO can still be improved. For instance, no meteor deceleration has been taken into account so far. Also the choice of a set of reference lightcurves to be preferentially adopted would deserve some further work. Moreover, it is known that the number of secondary bursts can well be higher than one in real events, and this also should be taken into account in future improvements of the model.

### 5.2 Meteor detection simulations: triggering and recording

The simulations of meteor events described above provide the input for the next necessary step of the analysis, namely a simulation of the response of the on-board electronics for the purposes of identification and recording.

Currently, the response of the detector, including optics and focusing, and the response of the photomultipliers in the focal surface, is parameterized. An overall throughput efficiency of 10 % is assumed. An optical point spread function (PSF) of $\sim$ 2.5 mm is assumed. Cross-talk, pixel-to-pixel response non-uniformity is of the order of 10 %. Poisson fluctuations of the night glow background are also introduced in the simulations. The FS is considered to be a uniform layer of MAPMTs (the gaps between tubes are ignored).

Due to the fact that the meteor luminosity can span over several orders of magnitude, different modes of detection must be designed. In particular, both acquisitions in single photon counting mode and acquisition in charge integration mode have to be planned. The single photon-counting technique has been developed mainly for cosmic rays observation, in which the maximum intensity of the signal is expected to be of the order of few tens of photo-electrons per pixel in one GTU. At higher rates, the photon-counting technique is affected by pile-up, and charge integration is therefore needed. Table 2 summarizes the relation between meteor absolute magnitude, photon flux, number of photo-electrons at the maximum of the development, mass and expected number of events in the field of view of JEM-EUSO in nadir mode. One should note that the definition of absolute magnitude for meteors, namely

**Table 2** For different absolute magnitudes (M) of meteors in visible light, the corresponding flux in the $U$-band are shown (according to the Flux Density Converter of the Spitzer Science Center; details can be found at the web site http://ssc.spitzer.caltech.edu/warmmission/propkit/pet/magtojy/index.html)

| Magnitude (M) | U-band flux (erg/s/cm$^2$/A) | Photons ($s^{-1}$) | Photo-electrons (GTU=2.5$\mu$s)$^{-1}$ | Mass (g) | Collisions in JEM-EUSO FoV |
|---|---|---|---|---|---|
| 7 | $6.7{\cdot}10^{-12}$ | $4.3{\cdot}10^{7}$ | 4 | $2{\cdot}10^{-3}$ | 1/s |
| 5 | $4.2{\cdot}10^{-11}$ | $2.7{\cdot}10^{8}$ | 23 | $10^{-2}$ | 6/min |
| 0 | $4.2{\cdot}10^{-9}$ | $2.7{\cdot}10^{10}$ | 2300 | 1 | 0.27/orbit |
| −5 | $4.2{\cdot}10^{-7}$ | $2.7{\cdot}10^{12}$ | $2.3{\cdot}10^{5}$ | 100 | 6.3/year |

The corresponding number of photons per second, the number of photo-electrons per GTU, the typical mass of the meteor, and the number of events expected to be observed by JEM-EUSO (the latter is computed assuming a duty cycle of 0.2) are also shown

the apparent brightness measured if the meteor was seen from the ground at a distance of 100 km in the zenith implies that the corresponding brightness as seen from JEM-EUSO will be fainter, because the ISS is located at an height of 400 km. A meteor located at an height of 100 km above the ground will be seen from a distance of 300 km from JEM-EUSO (assuming that the meteor has the ISS at the zenith). If the meteor has an absolute magnitude $M$, the corresponding apparent magnitude measured by JEM-EUSO will be therefore approximately $M_{app} = M + 2.4$.

In case of particularly bright meteors, a switch automatically reduces the high voltage level to reduce the collection efficiency of the MAPMT, limiting the intensity of the signal. In this way, saturation problems are avoided and a dynamic range of $10^6$ is guaranteed.

The most significant difference between single-photon counting and charge-integration modes is the pixel size. In fact, in case of charge-integration, pixels are grouped in bunches of 8 units (named KIs) to reduce memory resources. Figure 4 shows the currently assumed KI grouping (2×4 pixels).

Despite the fact that at high (faint) magnitudes meteor signals are comparable in luminosity to air showers produced by cosmic rays, their time duration is longer by orders of magnitude: seconds compared to hundreds $\mu$s in case of air showers. Therefore, to collect and properly record meteor events, some trade-off is needed because of the extremely high sampling rate of JEM-EUSO (2.5 $\mu$s). Such high time resolution would be in itself quite interesting, because some events could be acquired at least partially with such a high time-resolution. However, as this is not strictly necessary, it is convenient to assume in a conservative way that the light profile has to be sampled in order to reduce the recorded signal size of the event at a level comparable to air shower events ($\sim$ 300 kbytes).

In case of bright meteors, the acquisition is performed using only 288 KI channels per PDM. This is a factor 8 smaller than photon-counting pixels (2304 channels) used for fainter meteors, so that a slightly denser sampling becomes possible. In the case of KI, we can assume that in most cases we can acquire a total of 1024 GTUs sampled at a rate of one every 1024 GTUs (= 2.56 ms), giving a corresponding total time of 1024 × 1024 GTU = 2.6 s, which is in general sufficient to fully cover a

typical meteor track. In this way, the data budget for one event is $\sim$ 300 kbytes (288 channels $\times$ 1 byte/channel $\times$ 1024 GTUs). Of course, for bright fireballs, which can last longer, up to about 5 seconds, the observing strategy can be suitably tuned to be able to cover the entire time span of the event by changing the sampling rate and/or allocating a larger data budget. On the other hand, in case of high magnitude (fainter) events where photon-counting pixel mode is used, an equivalent solution is to acquire a total of 128 GTU with a sampling rate of one every 4096 GTU ($=$ 10.24 ms) for a total of 128 $\times$ 4096 GTUs $=$ 1.3 s. Even though the time span is shorter than in the previous case, it is sufficient to collect the visible part of the track. Naturally, the performance would improve if we could integrate the data in the GTUs instead of performing a sampling. This solution is under study, however, we consider here the most conservative case.

Of course, another important parameter is sky brightness. Moonlight is the largest background component. Figure 5 shows the observational duty cycle as a function of the accepted level of luminosity. In our study we assumed three different possibilities. One case corresponds to conditions of almost new moon, namely a background of $\sim$ 750 ph/m$^2$/ns/sr. The other two cases are characterized by higher background levels: $\sim$ 3000 ph/m$^2$/ns/sr and $\sim$ 7500 ph/m$^2$/ns/sr.

The trigger logic is defined following an approach similar to that adopted for air shower (cosmic ray) events. A detailed explanation of the trigger strategy for air showers is described in [12]. In the case of meteors, the first trigger level is issued if for a few consecutive GTUs, one KI channel detects an excess of signal, and such an excess, integrated along consecutive GTUs, is higher than a preset threshold. The

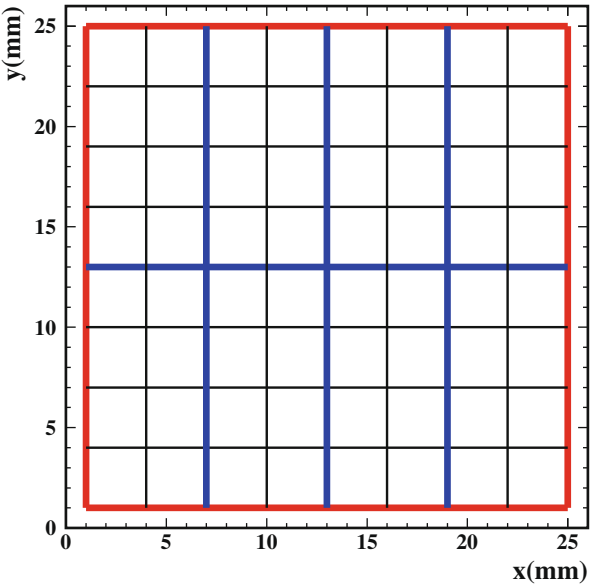


**Fig. 4** A schematic of a *M*64 Hamamatsu MAPMT is presented. The red line represents the MAPMT contour. The black squares are the MAPMT pixels used in photon-counting mode. The *blue grid* shows the assumed dimensions of the KI pixels, which are the pixels used in charge-integration mode

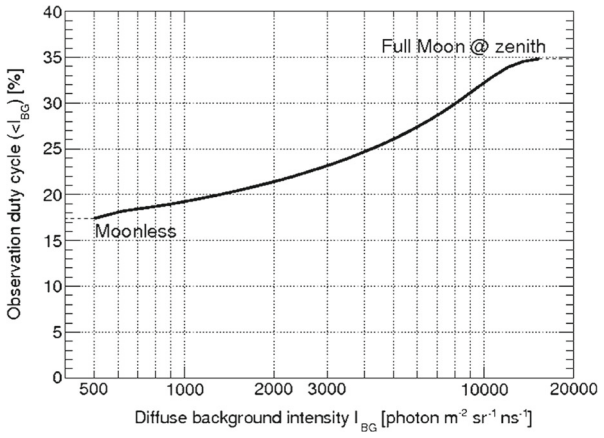


**Fig. 5** Observational duty cycle $\eta$ as a function of threshold background level $I_{\mathrm{BG}}^{\mathrm{thr}}$

threshold is set at a level such that Poisson fluctuations of the background rarely mimic this pattern, that is at a level of $\sim$ 1 Hz on the entire FS.

In case of much brighter meteors, the signal becomes too intense and it is necessary to reduce the collecting efficiency of the PMTs to avoid saturation problems. By means of switch logic, if the current produced at the anode exceeds a preset value, the collection efficiency on the first dynode is reduced in steps corresponding to a factor of 100. Information about the status of the switches is stored in memory in order to re-scale the data obtained in different conditions. In this way, the dynamic range of the measurement can be increased to cover 6 orders of magnitude in luminosity, corresponding to a range of 15 magnitudes.

### 5.3 The discrimination of anthropogenic lights

According to previous studies, city lights appear as objects of magnitude $M > 2$. As explained in Section 6, this class of sources will be detected by JEM-EUSO. Therefore, criteria must be established in order to exclude them from automated triggering procedures. Due to the ISS orbital velocity of $\sim$ 7 km/s, a fixed luminous spot on the Earth's ground produces a luminous track moving at the speed of the ISS, but in the opposite direction. As a first approximation, airplanes will also exhibit similar behaviour, as their speed is less than 0.3 km/s. A second trigger level is therefore needed to provide discrimination of anthropogenic sources. This is adapted from the procedure of detection for air showers produced by cosmic rays, which essentially follows the luminous spot on the PDM. The trigger logic can make a first guess of the apparent velocity and direction of the motion on the focal surface in order to verify whether it is compatible with a static source located on the ground.

In order to evaluate this possibility, we simulated a sample of meteors with magnitude $M = 2$ and differing velocities on the FS, and a sample of cities with different radii ($0 < \mathrm{R} < 10$ km) and a variety of magnitudes ($2.5 < \mathrm{M} < 4$). Figure 6 shows

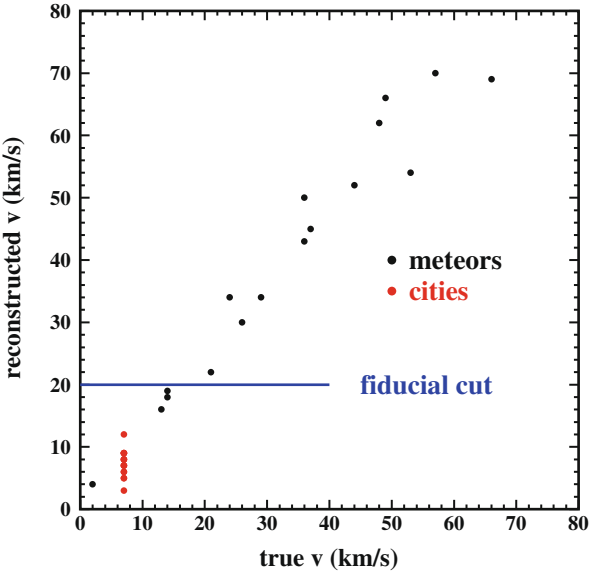


**Fig. 6** Scatter plot showing the projections on the FS of the true and reconstructed velocities for simulated meteors (*black dots*) and cities (*red dots*). A fiducial line to avoid triggering on cities based on the reconstructed projection of the velocity is also shown

a plot of the "true", velocities of simulated meteors and cities, and the velocities reconstructed by the trigger logic.

It is easy to see that the procedure of measurement of the source velocities works reasonably well. Moreover, cities, regardless of their brightness and size, exhibit low velocities. Therefore, a fiducial threshold can be placed on the reconstructed velocity at trigger level, to prevent from issuing a trigger driven by the detection of such low-velocity sources. In the specific case shown in the Figure, the fiducial line has been placed at a conservative value of 20 km/s. Of course, this threshold could be relaxed when flying above oceans, where the density of anthropogenic lights in the FoV is expected to be much smaller. Finally, this cut in velocity will be applied only for the range of meteorite magnitudes compatible with city lights, whose flux is sufficiently high ($\sim$ 1 ev/h in JEM-EUSO FoV). For much brighter objects, the recorded signal will be significantly higher and the fiducial threshold will not be required.

## 6 Preliminary results

A much simplified reconstruction algorithm has been applied to simulated meteor profiles in order to check the expected performances of the system. In particular, we have been studying the factors affecting the expected magnitude threshold for detection of these events in different background conditions in order to consistently apply either the analog or digital acquisition mode. A more refined technique is expected to be applied in the future that will improve the present results. We can therefore

consider current results to be fairly conservative. In the present approach, the signal from each pixel is acquired using the sampling technique explained in the previous Section, taking into account the detector response and background contribution. Three different photo-electron levels (16, 64, 160 photo-electrons/pix/GTU) corresponding to the background intensities of 750, 3000 and 7500 photons/$m^2$/sr/ns have been considered.

The procedure explained below is based on using KI pixels, but the same approach has also been applied to the case of digital pixels. First of all, the search for the meteor track on the FS is performed by selecting the KI pixel with the highest signal within each GTU. Figure 7 shows the selected pixels for the duration of a simulated meteor track having a magnitude $M = 2$, as well as the original track. During the brightest part of the meteor track, the correct pixels are selected and they appear to be aligned on a track as expected. However, in the first part of the meteor lightcurve, where the signal is still much fainter and background fluctuations dominate, pixels scattered over the entire portion of FS under consideration are selected. As a second step, a fit is performed on the detected part of the track, and is extrapolated to the rest of the track embedded in the noise. The average background level is then subtracted from all pixels.

Figure 8 shows the original light profile of the meteor, and the signal extracted using the reconstruction technique that we have just described. In order to determine the highest (that is, faintest) magnitude level at which the meteor profile could be reconstructed with reasonable uncertainties we have defined the following criteria:

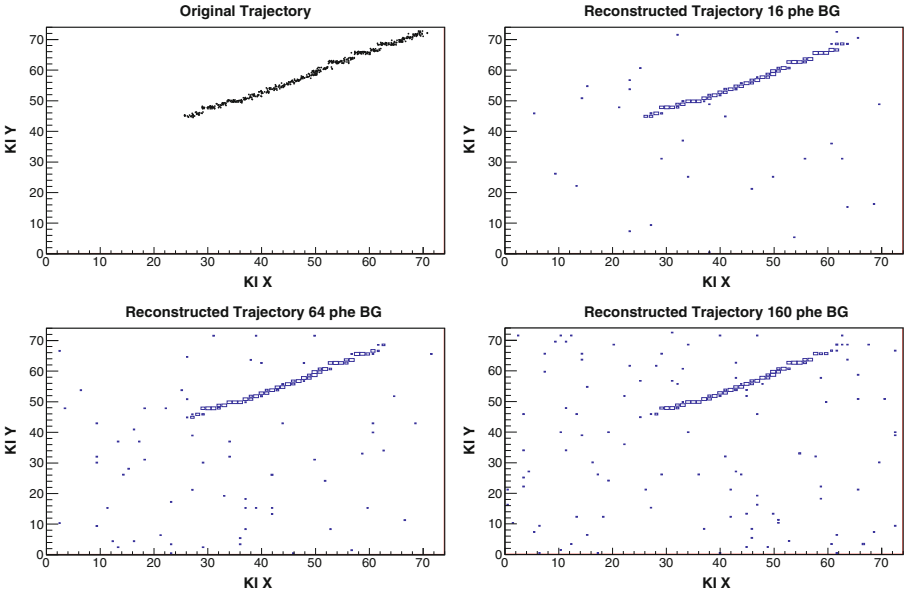


**Fig. 7** Original trajectory of a meteorite of magnitude $M = 2$ at pupil level, and the portion of the trajectory selected by the simple reconstruction technique described in the text for different background levels. For low background levels a longer track is reconstructed, as expected

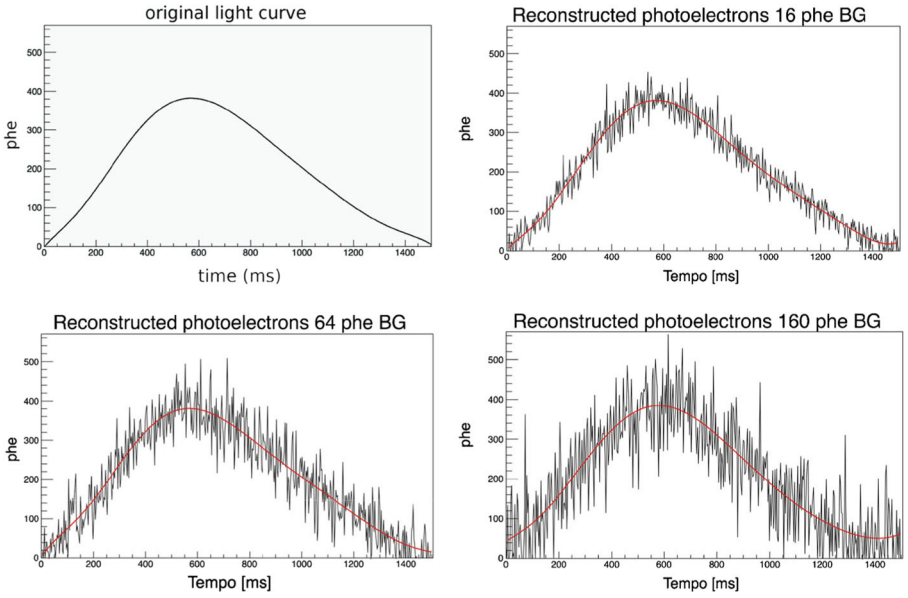


**Fig. 8** Original light profile of a meteor of magnitude $M = 2$ at pupil level, and the signal detected at FS level assuming different background levels as explained in the text

$$\Delta I = \frac{\int (\frac{\mathrm{d}phe}{\mathrm{d}t})_{rec} \cdot \mathrm{d}t - \int (\frac{\mathrm{d}phe}{\mathrm{d}t})_{true} \cdot \mathrm{d}t}{\int (\frac{\mathrm{d}phe}{\mathrm{d}t})_{true} \cdot \mathrm{d}t} \cdot 100(\%), \tag{4}$$

$$\Delta Max = \frac{Max_{rec} - Max_{true}}{Max_{true}} \cdot 100(\%), \tag{5}$$

where $\Delta I$ provides the resolution on the integrated lightcurve, while $\Delta Max$ gives an information on the uncertainty of the estimation of the peak of the light profile which is proportional to the magnitude of the event. The condition is that both the above parameters are reconstructed with uncertainties $\Delta I,\ \Delta Max < 20\ \%$. A quality cut on the shower profile is applied as well, to remove unsatisfactory reconstructions according to the above criteria.

Table 3 summarizes the results obtained for different background levels and magnitudes. This result shows that using KI information, the threshold for meteor observation is around magnitude 4 for low background levels and increases up to magnitude 2 for very high background conditions. Interestingly, we see that it is possible to detect and properly reconstruct meteor profiles at $M = +4$, for which the photon-counting technique starts to suffer from pileup (at the peak, $\sim 70$ phe/pixe/GTU as expected according to Table 2). Moreover, as the expected number of events in the FoV of JEM-EUSO is of the order of $\sim 1$ /min at this magnitude, it would be possible to record many of them during dark nights. Increased exposure time is required for brighter meteors such as $M = +2$ where the expected flux is expected to be $\sim 1$ ev/h.

For meteors of magnitude $M > 4$ photon-count mode is needed, rather than charge integration (KI). Because the smaller size of the pixels improves the signal to noise

**Table 3** Uncertainty on the reconstruction of $\Delta I$ and $\Delta Max$ for meteors of different magnitude and various background levels

| Background (phe/KI-pixel/GTU) | magnitude | $\Delta I$ (%) | $\Delta Max$ (%) |
|---|---|---|---|
| 16 | −1 | −0.2 | 0 |
| 16 | 0 | −0.1 | −0.4 |
| 16 | 1 | −1.6 | −1.1 |
| 16 | 2 | −5.7 | −3.5 |
| 16 | 3 | −0.1 | −2.2 |
| 16 | 4 | −19.5 | −10.7 |
| 64 | −1 | 0.7 | 0.3 |
| 64 | 0 | −0.2 | −0.4 |
| 64 | 1 | 3.9 | 1.7 |
| 64 | 2 | 0.7 | −0.4 |
| 64 | 3 | 11.3 | 5.0 |
| 160 | −1 | −1.1 | −0.8 |
| 160 | 0 | −7.5 | −3.9 |
| 160 | 1 | 5.8 | 3.2 |
| 160 | 2 | 1.9 | 0.5 |

ratio, photon-counting mode becomes more reliable. Figure 9 shows an example of reconstruction of the signal of a meteorite of $M = +5$ obtained by adopting the photon-counting sampling mode as described in the previous Section. The reconstructed meteor lightcurve proves a reasonable fit of the "true", simulated signal. A more detailed study indicates that the threshold level is around $M = +5.5$ if the sampling technique described in Section 5.2 is adopted. We have also seen in our

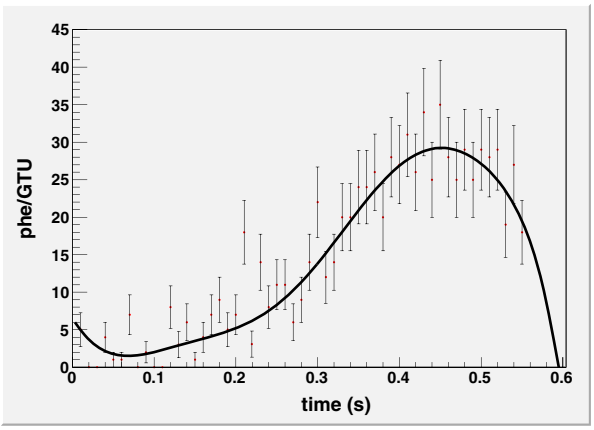


**Fig. 9** Reconstructed light profile of a meteor of magnitude $M = +5$ at pupil level detected in photon-counting mode

simulations that, by using a 25 $\mu$s GTU, it would be possible to push the sensitivity threshold for meteors around $M = +7$.

### 6.1 Nuclearites

The results already obtained for meteors can be used to draw some general and preliminary conclusions also for the nuclearites.

First of all, the detection sensitivity to nuclearites can be extrapolated from previous results obtained for the meteors. In particular, the absolute visual magnitude (M) of an atmospheric nuclearite located at 100 km distance can be computed according to [17] as:

$$M_{app} = 15.8 - 1.67 \cdot \log_{10}(m/1\,\mu\text{g}). \tag{6}$$

We recall that the absolute magnitude of a meteor corresponds to the apparent magnitude measured on the ground if the meteor is seen at the zenith and at an height of 100 km. By inverting (6) it is possible to estimate the minimum mass of the nuclearite detectable by JEM-EUSO in terms of absolute magnitude, which is independent of the distance $h$. This is reasonable at a first level of approximation, because the maximum difference of apparent magnitudes of the same event in different locations of the field of view is $\Delta M_{app} < 1$. Results indicate that JEM-EUSO is sensitive to objects having mass $m > 0.1$ g when working in single photon-counting mode, and to $m > 3 - 30$ g when working in charge integration mode. There is of course a dependence upon the sky background luminosity (mainly due to Moon phase).

For factors concerning the triggering strategy adopted for these events, the same algorithms already developed for meteors can be used, simply varying the total sampling time to take into account the shorter duration of the phenomenon (and correspondingly shorter track length). In the worst case scenario, a nuclearite starts to emit at an height of 60 km, moving along a trajectory with a zenith angle such that the track crosses the entire PDM along its diagonal ($\sim$ 42 km). Before impacting the ground, taking into account a velocity of 250 km/s, it follows that the total duration of the phenomenon is only $\sim$ 0.3 s. Therefore, in charge integration mode (KI mode) the optimized condition would be to record the signal during 1024 GTUs, sampled at a rate of one every 128 GTUs, whereas in single photon counting mode, one should record 128 GTU, with a sampling rate of one every 1024 GTUs. In both cases the total integrated time is $\sim$ 0.33 s (one GTU being equal to 2.5 $\mu$s).

The easiest way to distinguish nuclearites from meteors is by their velocity. Meteors have much slower speeds (in general below 72 km/s). As shown in Fig. 6, already at trigger level it is possible to estimate the projected velocity of the signal on the FS with reasonable uncertainty. Subsequent data analysis of the recorded signals carried out later on the ground will certainly provide much more accurate results. Although it is not possible to directly derive from the data the 3D velocity vector of the source, a limit can be set to the recorded projected velocity ($v_{proj}$). By requiring that $v_{proj} > v_{proj}^{min}$ and assuming that the velocity of the nuclearite is $v = 250$ km/s, choosing a value for $v_{proj}^{min}$ automatically sets a limit on the zenith angle of the track

**Table 4** Impact on the relative acceptance ($R_{acc}$) (see text) as a function of different possible choices of $v_{proj}^{min}$

| $v_{proj}^{min}$ (km/s) | $\theta_{min}$ (deg.) | $R_{acc}$ (%) |
|---|---|---|
| 100 | 23.6 | 84 |
| 130 | 31.3 | 73 |
| 160 | 39.8 | 59 |
| 190 | 49.5 | 42 |
| 220 | 61.6 | 23 |

$\theta_{min} = \arcsin(v_{proj}^{min}/v)$ and relative acceptance $R_{acc} = (1+\cos(2\cdot\theta_{min}))/2$. Table 4 shows the relative acceptance as a function of $v_{proj}^{min}$. It is clear that even a very tight cut on $v_{proj}^{min} > 160\,\mathrm{km/s}$ causes the acceptance to decrease only by about a factor of 2.

Another important fact to be considered is that nuclearites tend to develop at lower heights in the atmosphere compared to meteors. Moreover, any possible evidence of tracks moving upwards are a clear sign of a nuclearite. The light profile looks also quite different (see Fig. 10). It is not clear whether the large difference in velocity between nuclearites and meteors may explain *per se* at least in part why the detection of events to be possibly associated with nuclearites have not been so far announced

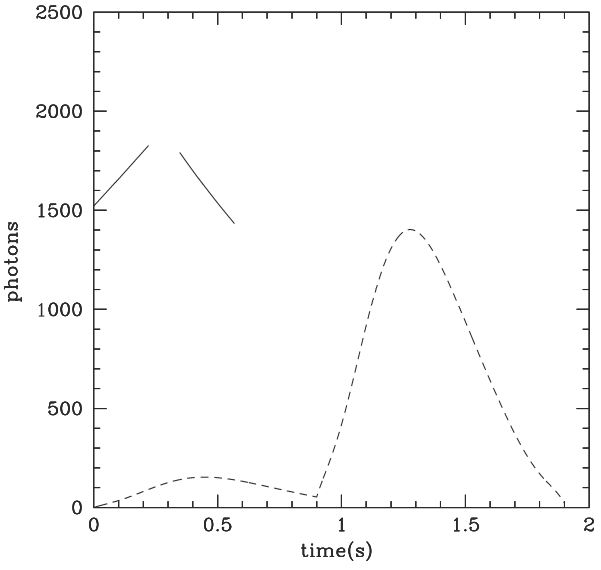


**Fig. 10** Comparison between the light profile of two nuclearites (*thick lines*) and that of a meteor (*dashed line*). The nuclearite has a mass of $m = 20$g and velocity of 250 km s$^{-1}$ and it is simulated up-ward going (*left curve*) and down-ward going (*right curve*) with $\theta = 45°$ inclination from the vertical. The magnitude of the meteor is M $= -1$, velocity 70 km s$^{-1}$, and $\theta = 45°$ inclination as well

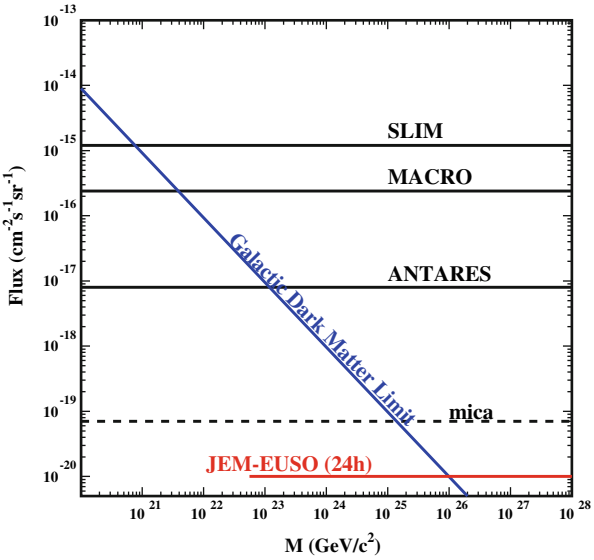


**Fig. 11** The JEM-EUSO 90 % confidence level upper limit on the flux of nuclearites resulting from null detection over 24 hours of JEM-EUSO operations. The limits of other experiments [3], [13], [32], [34] are also shown for a comparison. The old mica limits [34] are dependent on several additional assumptions, with respect to the other experiments

by ground-based meteor observers. There is the possibility that the brightness of these events could be generally lower than the values we have considered in our simulations. Coupled with their short durations, this could make the detection of these events particularly challenging. Of course, there is also the possibility that these events are extremely rare, or simply not existent.

We can expect therefore that JEM-EUSO will set very stringent limits on the flux of nuclearites even after short acquisition times, due to the tremendous instantaneous exposure (A $\sim$ 5 $\times$ $10^{20}$ cm$^2$ s sr) of the instrument. Even adopting a very severe rejection criterion, such as $v_{proj}^{min} > 190$ km/s, from Table 4 we can infer that for a 24 h accumulation time, a null detection would set a limit in flux at the 90 % confidence level of the order of $10^{-20}$ /cm$^2$/s/sr (see Fig. 11).

## 7 Conclusions and perspectives

Our preliminary analysis shows that JEM-EUSO has the capability to observe meteors down to magnitude $M < 5 - 6$, which could be reduced to $M < 7$ using a 25 $\mu$s GTU. Taking advantage of its large field of view and high detection rate, JEM-EUSO is able to record a statistically significant flux of meteors as a function of their magnitudes, both for what concerns sporadic meteors, and in cases of different meteor streams. Unaffected by adverse weather conditions, which limit the effectiveness of ground-based meteor observation networks, JEM-EUSO will become a very important facility in the field of meteor studies. A particularly important role can be played

in the detection of bright meteors and fireballs, as these events can be detected even during periods of very high sky background. Therefore, monitoring of these events can always be active, whereas the detection of faint meteors requires more optimal observing conditions, when the primary activity of the detectors is the observation of extremely energetic cosmic rays.

An exciting development to be explored is the possibility that in some cases, bright meteors may exhibit signal persistence. In the simulations carried out so far, it has been assumed that the signal is instantaneous and lasts for a time much shorter than the time step adopted in the simulations (0.001 sec). However, in the case of bright meteors this might be not realistic. If a meteor is so bright that it produces signals lasting over non- negligible time periods, it might be possible to exploit the movement of the ISS in order to derive at least a rough 3D reconstruction of the meteor trajectory. This, would allow the position and velocity vectors to be computed instead of a simple 2D projection of the motion. When possible, this would be a strong improvement, though it is limited to a small fraction of bright events.

Our preliminary analysis concerning the possible detection of nuclearites indicates that JEM-EUSO will be sensitive to nuclearites with mass higher than a few $10^{22}$ GeV/c$^2$. In addition, after a run time of only 24 hours, it will be able to provide limits on nuclearite flux one order of magnitude lower than the limits of the experiments carried out so far.

**Acknowledgments** This work was partially supported by the Italian Ministry of Foreign Affairs, General Direction for the Cultural Promotion and Cooperation. Discussions with some meteor experts, including Jiri Borowicka, Pete Jenniskens and Jeremy Vaubaillon were helpful and stimulating. The intelligent comments of two anonymous referees led also to major improvements of our original manuscript.

## References

1. Adams, J.H. Jr., et al., (JEM-EUSO Coll.): An evaluation of the exposure in nadir observation of the JEM-EUSO mission. Astropart. Phys. **44**, 76–90 (2013)
2. Alcock, C., Olinto, A.: Exotic phases of hadronic matter and their astrophysical application. Ann. Rev. Nucl. Part. Sci. **38**, 161–184 (1988)
3. Ambrosio, M., et al., (MACRO Coll.): Nuclearite search with the MACRO detector at Gran Sasso. Eur. Phys. J. C. **13**, 453–458 (2000)
4. Astone, P., et al.: Upper limit for nuclearite flux from the Rome gravitational wave resonant detectors. Phys. Rev. D **47**, 4770–4773 (1993)
5. Babadzhanov, P.B., et al.: Near-Earth object 2004CK39 and its associated meteor showers. MNRAS **420**, 2546–2550 (2012)
6. Babadzhanov, P.B., et al.: Near-Earth asteroids among the Scorpiids meteoroid complex. Astron. Astrophys. **556**, A25 (2013)
7. Baudis, L.: Talk at the Neutrino 2012 conference Kyoto Japan (2012)
8. Bertone, G., Hooper, D., Silk, J.: Particle dark matter: evidence, candidates and constraints. Phys. Rept. **405**, 279–390 (2005). arXiv:[hep-ph/0404175]
9. Blaizot, J.P., Iliopoulos, J., Madsen, J., Ross, G.G., Sonderegger, P., Specht, H.J.: CERN-2003-0001 (2003)
10. Bland, P., et al.: The Australian desert fireball network: a new era for planetary science. Aust. J. Earth Sci. **59**, 177–187 (2012)
11. Brown, P., et al.: A 500-kT airburst over Chelyabinsk and an enhanced hazard from small impactors. Nat. **503**, 238–241 (2013)

12. Catalano, O., et al., (JEM-EUSO Coll.): The trigger system of the JEM-EUSO telescope. In: Proceedings 31th Intenational Cosmic Ray Conference, vol. 5, pp. 1049–1052 (2009)
13. Cecchini, S., et al., (SLIM Coll.): Results on the search for strange quark matter and Q-balls with the SLIM experiment. Eur. Phys. J. C. **57**, 525–533 (2008)
14. Ceplecha, Z., et al.: Meteor phenomena and bodies. Space Sci. Rev. **84**, 327–471 (1998)
15. Ceplecha, Z., et al.: Superbolides. In: Meteoroids 1998, Proceedings of the International Conference, Tatranska Lomnica, Slovakia, 17–21 August 1998. Astronomical Institute of the Slovak Academy of Sciences, p. 37 (1999)
16. Dar, A., De Rujula, A., Heinz, U.W.: Will relativistic heavy ion colliders destroy our planet? Phys. Lett. B **470**, 142–148 (1999)
17. De Rujula, A., Glashow, S.L.: Nuclearites - a novel form of cosmic radiation. Nat. **312**, 734–737 (1984)
18. Ebisuzaki, T., et al., (JEM-EUSO Coll.): The JEM-EUSO project: observing extremely high energy cosmic rays and neutrinos from the international space station. Nucl. Phys. B (Proc. Suppl.) **175**, 237–240 (2008)
19. Gorham, P.W.: Antiquark nuggets as dark matter: new constraints and detection prospects. Phys. Rev. D **86**, 123005/1–8 (2012)
20. Gruen, H., et al.: Properties and interactions of interplanetary dust. In: Proceedings of the 85th Colloquium, Marseille, France, 9–12 July 1984 (A86-42326 20-90), p. 105. Reidel, Dordrecht (1985)
21. Han, K., et al.: Search for stable strange quark matter in lunar soil. Phys. Rev. Lett. **103**, 092302 (2009)
22. Herrin, E.T., Rosenbaum, D.C., Teplitz, V.L.: Seismic search for strange quark nuggets. Phys. Rev. D **73**, 043511/1-7 (2006). arXiv:[astro-ph/0505584]
23. Jenniskens, P., Vaubaillon, J.: Minor. Astron. J. **136**, 725–730 (2008)
24. Jenniskens, P., et al.: Almahata Sitta (=asteroid 2008 TC3) and the search for the ureilite parent body. MAPS **45**, 1590–1617 (2010)
25. Labun, L., Birrell, J., Rafelski, J.: Compact ultra dense matter impactors. Phys. Rev. Lett. **110**, 111102 (2013)
26. Lawson, K.: Quark matter induced extensive air showers. Phys. Rev. D **83**, 103520/1–9 (2011)
27. Kajino, F., et al.: The JEM-EUSO mission to explore the extreme Universe. Nucl. Instrum. Methods A **623**, 422–424 (2010)
28. Kusenko, A., Kuzmin, V., Shaposhnikov, M.E., Tinyakov P.G.: Experimental signatures of supersymmetric dark matter Q balls. Phys. Rev. Lett. **80**, 3185–3188 (1998). arXiv:[hep-ph/9712212]
29. Rietmeijer, F. Meteorit. Planet. Sci. **35**, 1025–1041 (2000)
30. Oberst, J., et al.: The "European fireball network": current status and future prospects. Meteorit. Planet. Sci. **33**, 49–56 (1998)
31. Ortiz, J.L., et al.: Detection of sporadic impact flashes on the Moon: implications for the luminous efficiency of hypervelocity impacts and derived terrestrial impact rates. Icarus **184**, 319–326 (2006)
32. Pavalas, G.E., et al., (ANTARES Coll.): Search for massive exotic particles with the ANTARES neutrino telescope. In: Proceedings of the 23rd European Cosmic Ray Symposium, Moscow, 543 (2012)
33. Pecina, P.G., Koten, P.: On the theory of light curves of video-meteors. Astron. Astrophys. **499**, 313–320 (2009)
34. Price, P.B.: Limits on contribution of cosmic nuclearites to galactic dark matter. Phys. Rev. D **38**, 3813–3814 (1988)
35. Proud, S.R.: Reconstructing the orbit of the Chelyabinsk meteor using satellite observations. Geophys. Res. Lett. **40**, 3351–3355 (2013)
36. Takahashi, Y., et al.: The JEM-EUSO mission. New J. Phys. **11**, 065009/1–21 (2009)
37. Trigo-Rodriguez, J.M., et al.: The development of the Spanish fireball network using a new all-sky CCD system. Earth Moon Planet. **95**, 553–567 (2004)
38. Trigo-Rodriguez, J.M., et al.: Asteroid 2002NY40 as a source of meteorite-dropping bolides. MNRAS **382**, 33–39 (2007)
39. Trigo-Rodriguez, J.M., et al.: Determination of meteoroid orbits and spatial fluxes by using high-resolution all-sky CCD cameras. Earth Moon Planet. **102**, 231–240 (2008)
40. Weryk, R.J.: The Southern Ontario all-sky meteor camera network. Earth Moon Planet. **102**, 241–246 (2008)

41. Witten, E.: Cosmic separation of phases. Phys. Rev. D **30**, 272–285 (1984)
42. Younger, J.P., et al.: A southern hemisphere survey of meteor shower radiants and associated stream orbits using single station radar observations. MNRAS **398**, 350–356 (2009)
43. Zigo, P., et al.: The activity and mass distribution of the Geminid meteor shower of 1996-2007 from forward scatter radio observations. Contrib. Astron. Obs. Skalnaté Pleso **39**, 5–17 (2009)